Published in final edited form as:
J Immunol. 2008 June 15; 180(12): 8444–8454.

CD4+ T Cells Target Epitopes Residing within the RNA-Binding Domain of the U1-70-kDa Small Nuclear Ribonucleoprotein Autoantigen and Have Restricted TCR Diversity in an HLA-DR4-Transgenic Murine Model of Mixed Connective Tissue Disease[1]

Eric L. Greidinger[*,†], **Yun Juan Zang**[*], **Kimberly Jaimes**[*], **Laisel Martinez**[†], **Mehdi Nassiri**[‡], and **Robert W. Hoffman**[2,*,†,§]

[*]Division of Rheumatology and Immunology, Department of Medicine, Miller School of Medicine, University of Miami, Miami, FL 33101

[†]Miami Veterans Affairs Medical Center, Miami, FL 33125

[‡]Department of Pathology, Miller School of Medicine, University of Miami, Miami, FL 33101

[§]Department of Microbiology and Immunology, Miller School of Medicine, University of Miami, Miami, FL 33101

Abstract

Mixed connective tissue disease (MCTD) is a systemic autoimmune disease with significant morbidity and premature mortality of unknown pathogenesis. In the present study, we characterized U1-70-kDa small nuclear ribonucleoprotein (70-kDa) autoantigen-specific T cells in a new murine model of MCTD. These studies defined 70-kDa-reactive T cell Ag fine specificities and TCR gene usage in this model. Similar to patients with MCTD, $CD4^+$ T cells can be readily identified from 70-kDa/U1-RNA-immunized HLA-DR4-transgenic mice. Using both freshly isolated $CD4^+$ T cells from spleen and lung, and T cell lines, we found that the majority of these T cells were directed against antigenic peptides residing within the RNA-binding domain of 70 kDa. We also found that TCR-β (TRB) V usage was highly restricted among 70-kDa-reactive T cells, which selectively used TRBV subgroups 1, 2, 6, 8.1, 8.2, and 8.3, and that the TRB CDR3 had conserved sequence motifs which were shared across different TRBV subgroups. Finally, we found that the TRBV and CDR3 regions used by both murine and human 70-kDa-specific $CD4^+$ T cells were homologous. Thus, T cell recognition of the 70-kDa autoantigen by HLA-DR4-transgenic mice is focused on a limited number of T cell epitopes residing primarily within the RBD of the molecule, using a restricted number of TRBV and CDR3 motifs that are homologous to T cells isolated from MCTD patients.

Mixed connective tissue disease (MCTD)[3] is a systemic autoimmune disease characterized immunologically by the presence of autoantibodies reactive with U1 ribonucleoprotein (U1-RNP) polypeptides, including the U1-70-kDa (70-kDa) polypeptide, and their associated

[1]This work was supported by grants from the National Institutes of Health, Lupus Foundation of America, Lupus Research Institute, and Department of Veterans Affairs.

[2] Address correspondence and reprint requests to Dr. Robert W. Hoffman, Division of Rheumatology and Immunology, University of Miami, 1120 N.W. 14th Street (D4-10), Miami, FL 33136. rhoffman@med.miami.edu.

Disclosures: The authors have no financial conflict of interest.

[3]Abbreviations used in this paper: MCTD, mixed connective tissue disease; RNP, ribonucleoprotein; SLE, systemic lupus erythematosus; RBD, RNA-binding domain; Tg, transgenic; TRB, TCR-β; MC, medium control.

U1-RNA (1). Clinically, MCTD is characterized by manifestations that overlap systemic lupus erythematosus (SLE), scleroderma, inflammatory myopathy, and rheumatoid arthritis (2,3). The primary disease-related cause of death in MCTD is pulmonary disease including pulmonary hypertension, which distinguishes it from SLE where pulmonary disease is uncommon (4).

The putative target of autoimmunity in MCTD is the U1-RNP Ag which is a U1-RNA-small nuclear RNP complex that is normally contained within the nucleus of eukaryotic cells and whose biologic function is to convert pre-mRNA to mature mRNA (5–7). The 70-kDa polypeptide of the U1-RNP Ag is a dominant autoantigen in MCTD and consists of a 437-residue polypeptide which noncovalently associates with U1-RNA through an RNA-binding domain (RBD) on the polypeptide spanning residues 92–202 (8).

In a recent genome-wide association study, we found that genetic association of MCTD with the MHC which is consistent with previous candidate gene studies where association of MCTD with *HLA-DRB1*04* alleles was found (2,9,10). Furthermore, HLA-DR4-restricted $CD4^+$ T cells reactive with U1-RNP polypeptides including 70 kDa have been isolated from PBMC of MCTD and characterized in considerable detail (11–14). We have shown that these human $CD4^+$ T cells can provide help to anti-70-kDa autoantibody producing B cells, are restricted in Ag presentation by HLA-DR, have TCR fine specificity for peptides encoded within the RBD of 70 kDa, and have limited TCR-β (TRB) V and CDR3 usage (11–17).

To further advance our current understanding of the pathogenesis of MCTD, we have developed a model of MCTD in mice that expresses a transgene (Tg) encoding the HLA-DR4 molecule (HLA-DRA*0101/DRB1*0401) by immunizing them with the p205 fusion protein of the 70-kDa polypeptide and its associated U1-RNA (18). These mice develop sustained anti-U1-RNP Abs following a single exposure to the 70-kDa polypeptide/U1-RNA autoantigen (19–21). Further distinguishing the model, these mice develop pulmonary inflammatory infiltrates characteristic of MCTD but do not develop anti-Sm-Abs or anti-DNA Abs which distinguishes the model from SLE (2–4,21).

In the present study, we characterized the peptide-TCR molecular interactions of 70-kDa-reactive $CD4^+$ T cells in this novel model of MCTD, including characterizing the $CD4^+$ T cell Ag fine specificities and TCR usage in 70-kDa autoantigen recognition. We found that similar to patients with MCTD, $CD4^+$ T cells can be readily identified from HLA-DR4-Tg mice following a single exposure to 70-kDa/U1-RNA and that the majority of these T cells are specific for antigenic peptides encoded within the RBD of 70 kDa. Also similar to MCTD, we found by examining 70-kDa-specific T cell lines that TRBV usage was highly restricted among 70-kDa-reactive murine T cells. TCR from 70-kDa-reactive $CD4^+$ T cells demonstrated selective use of TRBV subgroups as well as common structural CDR3 motifs across different TRBV subgroups. Finally, we found that TRBJ subgroups and TRB CDR3 used by human and murine $CD4^+$ T cells were homologous.

Materials and Methods

Mice

C57BL/6Ntac-(KO)Abb-(Tg)DR-4 mice were purchased (Taconic Farms). The transgenic strain uses a hybrid MHC class II molecule composed of the peptide-binding domains of human HLA-DR4 and the membrane proximal domains of mouse I-E. Native MHC class II is not expressed as these have been genetically inactivated (I-E β and I-A α deficient). As the α2 and β2 domains of mouse MHC class II are preserved in the transgene, interactions with CD4 coreceptors on murine T cells are maintained (18). As previously reported the

HLA-DR4-Tg mice in our colony have not developed serologic or clinical manifestations of spontaneous autoimmunity at up to 9 mo of age (19,20).

70-kDa and U1-RNA Ags

Fusion protein for the 70-kDa Ag, as well as control maltose-binding protein, was produced and characterized as described previously (11,17,21). In brief, the p205 peptide of the 70-kDa protein, spanning amino acids 63–205, was expressed as a maltose-binding protein fusion protein in *Escherichia coli*, affinity purified over amylose columns and gel-purified. For ELISA studies, maltose-binding protein was cleaved from the 70-kDa peptide with Genenase (New England Biolabs), and the resulting 70-kDa product was gel-purified. The identity and purity of all products was confirmed by immunoblot against standard 70-kDa-recognizing sera, and each was confirmed for the absence of endotoxin contamination with a *Limulus* assay (Cambrex Bio Science). U1-RNA was produced by in vitro transcription of a Sp64 plasmid (Promega) containing a 165-base insert corresponding to the sequence of the human U1-RNA, as previously described (22). U1-RNA was tested for contamination with endotoxin as described above.

Immunization of mice

Mice were immunized s.c. once between 8 and 12 wk of age with 50 μg of a purified 70-kDa fusion protein containing 70-kDa residues 63–205 in 50 μl of PBS. Ags were instilled mixed with 50 μg of U1-RNA in 50 μl of sterile PBS. Blood and urine samples were collected immediately before immunization and monthly thereafter. Urine was tested for blood and protein using Multistix 10 SG Reagent Strips (Bayer). Except for animals that died or required euthanasia for humanitarian reasons before completion of the protocol, all mice were sacrificed at 2 mo after immunization. All mouse studies were approved by the Institutional Animal Care and Use Committee at the University of Miami Miller School of Medicine, and all animals were housed in American Association for Accreditation of Laboratory Animal Care-approved facilities.

ELISA

Anti-70-kDa and -maltose-binding protein assays were performed as previously described (4,19–21). Briefly, 96-well flat-bottom microtiter plates were incubated overnight at 4°C with purified Ag in PBS. After washing in PBS/0.05% Tween 20 buffer, plates were blocked with 3% powdered milk in PBS/Tween 20, incubated with mouse sera at final dilutions of 1/100, and developed with HRP-linked Fc region-specific goat anti-mouse-IgG secondary Ab followed by orthophenylenediamine. Absorbance at 450 nm was measured in a microtiter plate reader (Bio-Tek). Anti-dsDNA assays were performed using a commercial kit for murine dsDNA IgG (Alpha Diagnostic International), according to the manufacturer's instructions. All ELISA were performed in duplicate wells. Standard positive and negative control sera and test antisera were assayed on each plate.

Histology

Mice were euthanized by cervical dislocation after induction of anesthesia using isoflurane inhalation 2 mo after immunization, and organs were immediately harvested and fixed in UMFIX (20). Lungs were inflated with fixative at the time of harvest as previously described (20). Paraffin-embedded sections were stained using H&E or using a series of mAb, and imaged with a Nikon CoolPix 990 camera mounted on an Olympus BH2 microscope. All slides were graded at the same session, blinded to the mouse strain and immunization condition of the animals. Histologic assessments were confirmed by an additional independent blinded trained pathology review. For publication purposes, images

were cropped using Microsoft Powerpoint; no additional image manipulation was performed.

Peptide design and synthesis

Peptides were synthesized using *N*-[9-fluorenyl]methoxycarbonyl solid-phase chemistry on the AAPPTEC Apex 396 or the Applied Biosystems 433A model peptide synthesizer. Peptides were analyzed for purity and sequence fidelity using HPLC and mass spectrometry, as described previously (17).

T cell isolation

Cells were purified from spleen and lymph nodes by mechanical separation and passage through a 100-μm mesh filter (BD Biosciences). Cells were treated with RBC lysis buffer (Sigma-Aldrich), washed in RPMI 1640 with 2 mM L-glutamine, supplemented with 20 μg/ml gentamicin and 10% FCS, and then passed over Histopaque 1083 (Sigma-Aldrich) for further purification of lymphocytes. Cells were taken from the Histopaque interface and washed in RPMI 1640 followed by an additional wash in MACS buffer (Miltenyi Biotec). The cells were then incubated with anti-CD4 mAb (BD Biosciences) coupled to iron beads (Miltenyi Biotec) for 15 min in MACS buffer. Following incubation of the cell-Ab-bead conjugates, cells were positively selected on an AUTOMACS cell separator (Miltenyi Biotec) magnetic column and their purity was confirmed by flow cytometry; AUTOMACS isolation typically yielded $CD4^+$ T cells of >95% purity. Highly purified $CD4^+$ T cells were resuspended at the appropriate concentration and used in proliferation experiments as described below.

Murine lung T cell isolation

T cells were obtained at necropsy from lung tissue by mechanically disrupting the tissue, following which it was filtered through a sterile 100-μm nylon mesh filter and then subjected to density gradient centrifugation using Histopaque (Sigma-Aldrich). Purified CD4 cells were stimulated with plate-bound anti-CD3 and mRNA was isolated as described (16). All T cells studied were from mice with histologically confirmed pulmonary inflammatory infiltrates.

Murine T cell lines

Murine T cell lines used in these studies were generated and characterized using an approach similar to that which has been used extensively for generating human autoantigen-specific T cell lines and clones with slight modifications (11–13). In brief, spleen and lymph node cells were obtained at necropsy, mechanically disrupted, filtered through a sterile 100-μm nylon mesh filter and then subjected to density gradient centrifugation using Histopaque (Sigma-Aldrich). Cells obtained from immunized mice as responder cells were used immediately in proliferation or for the generation of T cell lines. Cells obtained from naive mice were irradiated with 30 Gy and used as APC to stimulate T cells and in proliferation assays. Approximately 5×10^6 cells were cultured in DMEM with 2 mM L-glutamine (complete medium), supplemented with 20 μg/ml gentamicin, 15% FCS, and containing fusion protein at a final concentration of 50 μg/ml. As Ag, 70-kDa fusion protein was used, as described (11–13,17). Cells in a final volume of 5 ml were placed in a 25-cm^2 flask and incubated in 5% carbon dioxide at 37°C. Cells were restimulated with 5×10^6 murine APC that had been irradiated with 30 Gy plus Ag in fresh medium on days 7–10. Following two cycles of stimulation, cells were rested for 10 days and then either tested in a standard proliferation assay or stimulated with plate-bound anti-CD3 with 20 U/ml IL-2 in complete medium and used for TCR analysis. RNA was extracted from the cells which had been

stimulated with plate-bound anti-CD3 in the absence of APC at 48 h for TCR analyses using RNeasy (Invitrogen).

Proliferation assay

Approximately 2×10^4 $CD4^+$ T cells from immunized mice were cultured with ~1×10^5 APC in complete medium. APC were obtained from naive DR4-Tg mice which had been irradiated with 30 Gy. T cells and APC were subsequently incubated for 48 h in 96-well flat-bottom tissue-culture plates in the presence of Ag or medium control (MC). Cells were then pulsed for an additional 18 h with 1 μCi/well [^{3}H]TdR. Cells were harvested and [^{3}H]TdR incorporation detected by liquid scintillation counting (17).

Flow cytometry

The TRBV expression on T cells was identified using flow cytometry and a series of group-specific mAbs (mouse VB TCR screening panel, Technical Bulletin 557004, www.bdbiosciences.com and Ref. 23). Briefly, following density gradient separation cells were stained using mAb specific for TCR VB 2, 3, 4, 5.1, 5.2, 6, 7, 8.3, 9, 10, 11, 12, 13, 14, and 17a (BD Biosciences) and counterstained with anti-CD4-PE (BD Biosciences). Isotype controls were conjugate coupled IgG2b (BD Biosciences) and IgG2b (BD Biosciences). Cells were enumerated on a LSRII cytometer and results were analyzed using FACSDiva software (BD Biosciences). Following initial gating on the lymphocyte population, cells were enumerated for those which were $CD4^+$ with each of the group-specific TRBV mAbs. The absolute number of each cell subset was calculated based on the absolute number of $CD4^+$ cells and the total lymphocyte count.

PCR analysis of TCR

mRNA was extracted from cell pellets using an oligo(dT)-cellulose mi-croaffinity column adsorption method (MicroFastTrack 2.0; Invitrogen). First-strand synthesis of cDNA was conducted using reverse transcriptase and RNaseH (SuperScript First-Strand Synthesis System for RT-PCR; In-vitrogen Life Technologies). Aliquots of cDNA were PCR amplified in the presence of primers specific for 1 of 22 TRBV groups of the TCR (Table I) (15–17,23,24). As a positive control, the amplification of a portion of the TCR-α C region was conducted in parallel. As described previously, extensive precautions were taken to ensure that cross-contamination of samples did not occur (15–17). The amplified DNA was subjected to gel electrophoresis in 3% Nusieve, 1% SeaKem agarose and visualized by staining with ethidium bromide. PCR-amplified fragments were purified using the QIAquick PCR purification kit (Qiagen) and cloned into pCR-Blunt II-TOPO vector using the Zero Blunt TOPO PCR cloning kit with One Shot chemically competent *E. coli* (Invitrogen). DNA sequencing was performed as described previously (10,15–17).

GenBank accession numbers

Accession numbers assigned to novel TCR gene sequences identified in this study were EF457520-EF457550 and EU518945-EU519008.

Statistical analysis of data

The Graph Pad Prism software package was used to analyze data.

Results

70-kDa/U1-RNA-immunized HLA-DR4-Tg mice develop high-titer IgG anti-70-kDa autoantibodies following immunization

Following immunization with 70-kDa/U1-RNA, mice developed high-titer IgG reactivity with 70-kDa as detected by ELISA and immunoblotting. Fig. 1 illustrates the presence of IgG anti-70-kDa specific Abs as detected by immunoblotting of sera from 70-kDa/U1-RNA-immunized HLA-DR4-Tg mice. Shown are typical immunoblotting results using sera diluted 1/5000 from 70-kDa/U1-RNA-immunized HLA-DR4-Tg mice to probe Jurkat cell extract. Sera from immunized mice but not naive mice had high levels of specific IgG reactivity with the 70-kDa protein. The IgG reactivity against 70 kDa, as detected by immunoblotting and ELISA, was typically detectible within 1 mo following immunization and continued to rise over time with the highest levels present at the terminal bleeding of immunized mice.

70-kDa/U1-RNA-immunized HLA-DR4-Tg mice develop T cell infiltration of the lungs similar to MCTD

Fig. 2 illustrates the characteristic histologic findings in HLA-DR4-Tg mice immunized with 70-kDa/U1-RNA including the presence of substantial numbers of T cells (20). Fig. 2A illustrates H&E staining of representative lung tissue demonstrating the characteristic perivascular and interstitial mononuclear cell infiltration of the lung; Fig. 2B is a section corresponding to *A* which was stained with enzyme-coupled anti-CD3 illustrating immunohistochemical findings of $CD3^+$ T cell staining of lung tissue at sites of inflammation as seen on H&E staining. Fig. 2C illustrates a representative section of lung from a naive unim-munized HLA-DR4-Tg mouse showing the absence of significant tissue staining. This demonstrates that immunized HLA-DR4-Tg mice developed T cell-enriched perivascular and interstitial mononuclear cell infiltration of lung tissue similar to that found in involved human lung from MCTD patients (R. W. Hoffman, unpublished observations; and Refs. 2 and 3).

Immunized HLA-DR4 Tg mice develop 70-kDa-reactive $CD4^+$ T cells

To determine whether 70-kDa-reactive $CD4^+$ T cells could be detected from 70-kDa/U1-RNA-immunized mice, purified $CD4^+$ T cells were incubated with a series of pooled, overlapping peptides, 15 residues in length (shown in Table II), spanning the 70-kDa protein in the presence of irradiated syngeneic APC. [^{3}H]TdR incorporation was measured and a stimulation index calculated for each sample. $CD4^+$ T cells reactive with 70-kDa peptides could readily be detected in all mice studied. Representative results from three of six mice are shown in Fig. 3. Murine $CD4^+$ T cells proliferated consistently to pools 1, 4, 9, and 10, while individual mice variously responded to pools 5, 7, and 11. Although clear findings of $CD4^+$ T cell-proliferative responses to 70 kDa were obtained, the high background levels of proliferation of T cells from some mice made precise interpretation of T cell epitope mapping results difficult using the peptide pools.

70-kDa-reactive T cells target RBD on Ag

To confirm findings from experiments using pooled peptides and to more precisely determine the T cell epitopes recognized by $CD4^+$ T cells from immunized DR4-Tg mice, purified $CD4^+$ T cells were incubated with a series of individual peptides spanning the entire 70-kDa protein and overlapping each other in sequence, in the presence of irradiated syngeneic APC. [^{3}H]TdR incorporation was measured and results shown as stimulation indices. Representative results from three mice are shown in Fig. 4. These three representative results ($n = 6$) confirmed results from experiments using pooled peptides that

there were at least seven regions which could be reliably identified as reactive with $CD4^+$ T cells in immunized mice. The majority of T cell epitopes resided within the RBD (shown in brackets) of the 70-kDa protein. There were a limited number of T cell epitopes which resided in regions within either the N or C terminus of the 70-kDa protein and which were outside the RBD that were identified in some mice.

70-kDa epitope 2 is the most frequently recognized T cell epitope in immunized HLA-DR4-Tg mice

To further define the frequency of T cell epitope reactivity against different regions of 70 kDa in immunized HLA-DR4-Tg mice, we examined the T cell proliferative responses in a panel of 10 mice to the five dominant T cell epitopes previously identified in MCTD patients which were termed epitopes 1–5. Freshly isolated $CD4^+$ T cells from all mice demonstrated a proliferative response to 70-kDa Ag. As summarized in Table III, we found that similar to MCTD $CD4^+$ T cells from immunized mice recognized all five T cell epitopes within the RBD although with slightly different frequency than that found in the small group of MCTD patients previously studied (17).

TRBV subgroups use in $CD4^+$ T cells from 70-kDa-immunized mice is restricted to select TRBV subgroups and CDR3 usage appears nonrandom

We next examined TCR usage by T cells reactive with 70-kDa autoantigen in the context of HLA-DR4 in the Tg mice to determine whether TRBV usage by 70-kDa-reactive $CD4^+$ T cells was randomly distributed or showed discernable bias of either TRBV subgroup or CDR3 usage. Previously, we had found in MCTD patients that the TRBV gene usage in 70-kDa-specific $CD4^+$ T cell clones was not randomly distributed and that certain TRBV structural motifs were more common among patients compared with controls (16). To identify TRBV used by $CD4^+$ T cells in the MCTD murine model, we first performed two-color flow cytometry on T cells stained for CD4 that were also stained with individual mAbs specific for TRBV used by the C57BL/6 strain of mice: BV 2, 3, 4, 5.1, 5.2, 6, 7, 8.3, 9, 10, 11, 12, 13, 14, or 17. Table IV summarizes the TRBV gene usage for BV 2, 3, 4, 5.1, 5.2, 6, 7, 8.3, 9, 10, 11, 12, 13, 14, and 17 found using splenic T cells. Using flow cytometry to analyze TRBV genes from splenic T cells, it was observed that there were slight variations between immunized and naive mice with increases in TRBV 4 and 8.3 and decreases in TRBV6, 7, and 10, but these differences were not statistically significant for either the percentage or absolute number of $CD4^+$ T cells (Table IV).

We also examined TRBV used by T cells isolated from lymph nodes of immunized and control unimmunized mice and found no statistically significant differences (data not shown). Next, we performed RT-PCR using TRBV group-specific primers to examine TRBV usage compared with the flow cytometry results and to interrogate those TRBV subgroups where TCR group-specific mAbs were not available. Findings by RT-PCR were similar to those obtained by flow cytometry with no discernable expansion of any TRBV subgroup (data not shown). Although the difference between immunized and unimmunized mice was not statistically significant, such an approach at the bulk cell level might not be adequate to identify clonal expansion by a highly restricted set of T cells.

We next examined TRBV distribution from short-term $CD4^+$ T cell lines which were generated in vitro using 70-kDa Ag stimulation. Using this approach, we found that the short-term $CD4^+$ T cell lines selectively used TRBV1, VB2, VB6, and VB 8.1/8.2/8.3. We then cloned and sequenced TCR from these lines and found that the CDR3 were highly restricted (Table V), characteristic of an Ag-driven T cell response. As controls, randomly cloned and sequenced CDR3 from unselected $CD4^+$ T cells from spleen were examined.

Unlike the short-term T cell lines, T cells from unfrac-tionated whole spleen did not demonstrate any identifiable skewing of structural motifs or CDR3 length (data not shown).

TRBV use by $CD4^+$ T cells from 70-kDa-immunized HLA-DR4-Tg mice demonstrates homology to TCR use by human T cell clones from MCTD patients

To determine whether there was a relationship between TCR usage by 70-kDa-reactive human and murine T cells, we compared TRBV use by human $CD4^+$ T cell clones reactive with 70-kDa protein with those of TRBV derived from short-term $CD4^+$ T cell lines derived from HLA-DR4-Tg mice. As we have in part reported previously, sequences from 18 individual human T cell clones derived from patients with and without HLA-DR4 revealed three unique TRBV sequences (17). When these were compared with the unique murine $CD4^+$ TRBV sequences significant homology was identified (see Table VII). The murine sequences with the greatest homology are shown aligned to the human sequences and the regions of shared sequence identity are underlined (see Table VII). Also, it was notable that TRBJ2S7 was highly represented in both the human (7 of 18; 56%) and murine spleen (24 of 115; 21%) TCR identified.

TRBV use by $CD4^+$ T cells from 70-kDa-immunized HLA-DR4-Tg mouse lungs demonstrates homology to TCR use by murine splenic $CD4^+$ T cells

Although murine 70-kDa-specific T cell lines demonstrated TRBV and CDR3 homology with TCR from human 70-kDa-reactive T cell clones, it remained possible that this could be attributable to antigenic selection and expansion in vitro. To more directly address this possibility, $CD4^+$ T cells were isolated directly from the lungs of mice found to have pulmonary inflammation histologically (17). Lung tissue mRNA was extracted and TRBV usage was characterized by RT-PCR and DNA sequencing using group-specific primers. When the human sequences were compared with murine $CD4^+$ TRBV sequences from lung tissue, significant homology was identified (Tables VI and VII) (16). The murine sequences with the greatest homology are shown aligned to the human sequences and the regions of shared sequence identity are underlined (Table VII). As was seen in splenic tissue (TRBJ2S7 present in 24 of 115 (21%) of isolates), it was again notable that TRBJ2S7 was highly represented in both the human (7 of 18; 56%) and lung (19 of 81; 24%) TCR identified (Table VII).

Discussion

HLA-Tg mice immunized with a specific autoantigen have been reported as potentially powerful models for dissections of molecular interactions between defined autoantigen-MHC complexes and the TCR (18,25–28). Such an approach holds substantial promise for the detailed analysis of TCR-antigenic peptide-human MHC interactions in those unique instances where the autoantigen is known and structurally well-characterized such as MCTD.

We have developed a new murine model of systemic autoimmunity, using HLA-DR4-Tg mice, which is induced following a single immunization with the 70-kDa polypeptide of U1-RNP and its associated U1-RNA. Immunization induced high levels of IgG anti-U1-RNP Abs characteristic of MCTD which increased over time without additional boosting; however, these immunized animals did not develop anti-dsDNA or anti-Sm autoantibodies which are characteristic of SLE and are found in murine models of SLE (19,20).

In addition to the development of high titers of autoantibodies, 70-kDa/U1-RNA-immunized HLA-DR4-Tg mice develop additional features characteristic of MCTD. A distinguishing feature of the model is that mice develop pulmonary inflammation, including mononuclear

cell perivascular and interstitial infiltration of the lungs which typifies MCTD but is uncommon in SLE (2,3). Pulmonary infiltrates in mice contained a substantial proportion of lymphoid cells including T cells (Fig. 2). These finding are similar to those in pulmonary tissue in MCTD patients where T lymphocytes are prevalent (R. W. Hoffman, unpublished observations; and Refs. 2 and 3). Furthermore, in preliminary studies, we have found that adoptively transferred $CD4^+$ T cells alone or in conjunction with B cells can transfer disease to naive mice (29). While beyond the scope of the present report, this is currently an area of active investigation in our laboratory.

To more fully define the nature of the autoantigenic peptides recognized by $CD4^+$ T cells in the model, we have tested the proliferative responses of $CD4^+$ T cells isolated from immunized mice against a large panel of synthetic peptides spanning the 437-residue 70-kDa polypeptide (8,17). As shown in Figs. 3 and 4 and summarized in Table III, we found that the T cell proliferation could readily be detected using $CD4^+$ T cells from whole splenocytes and lymph nodes. T cell epitopes recognized by $CD4^+$ T cells from mice were similar to those previously identified in MCTD patients in that most resided within the RBD of 70 kDa (8). There was also limited immune spreading to T cell epitopes outside of those contained within the immunizing fragment of 70 kDa to residues contained within the N and C terminus of the full-length molecule. Thus, while immune spreading can occur, the T cell response in the murine model is similar to human MCTD and remains focused primarily on the RBD.

The importance of the RBD as a shared target of autoimmune B cell responses to complex nuclear Ags has been emphasized by Monneaux and Muller, and Mamula et al. (30,31). The RBD has also been identified as a dominant T cell epitope in nonautoim-mune-prone CBA normal mice immunized with 70 kDa, as well as in the MRL/*n* and MRL/*lpr* spontaneous murine models of SLE, and among T cells reactive with 70 kDa isolated from patients with MCTD (17,32,33). The mechanistic basis of T cell responses focusing on the RBD could reflect indirect influences of B cell epitope selection and Ag presentation to T cells, preferential Ag protection/processing of the RNA-RBD complex by dendritic cells or other APC, or other mechanisms (17,31). Interestingly, Muller and colleagues (33) have demonstrated that immune tolerance to 70 kDa can be restored in lupus prone mice through immunization using peptides derived from the RBD; therefore, understanding the molecular basis of these interactions may have important implications for future T cell directed therapy.

Toward the goal of further defining the molecular details of the interactions between the TCR and the 70-kDa autoantigen, TCR use by 70-kDa-reactive T cells was examined using several approaches. We discovered that TRBV usage by $CD4^+$ T cells was restricted to a select subgroup of TRBV genes (Tables V and VI) and that common structural motifs could be identified within the CDR3 across the different TRB subgroups identified. The use of selective *TRB* or *TRA* genes has been described in a number of autoimmune diseases including SLE, autoimmune thyroiditis, multiple sclerosis, ulcerative colitis, and polymyositis (14–16,34–38). These studies suggested that even for a structurally complex autoantigen, which has the potential to generate a large number of peptide-TCR interactions, the T cell response in these autoimmune diseases may be focused on a surprisingly limited number of epitopes and/or use a limited number of TCR motifs. When we compared the TRB and CDR3 from 70-kDa-reactive $CD4^+$ T cells in HLA-DR4-Tg mice with those we have previously identified from MCTD patients, we found striking similarities between TCR use in MCTD and the murine model (Table VII).

Few previous studies have been published examining detailed molecular interactions between an autoantigen and the TCR and even fewer have directly compared findings in the

murine model with human disease. One of the most striking findings of the present study was the fact that highly restricted *TRBV* genes used in the model were highly similar to those found in MCTD patients (Table VII) (16). Common TCR use of TRBV and select CDR3 in the model was homologous to TCR use in MCTD (16). The similarity of this and other aspects of the model to human disease validates its relevance to human disease pathogenesis and helps establish its potential future utility as a preclinical model for manipulation of T cell responses (39).

Acknowledgments

We gratefully acknowledge the excellent technical assistance of Judith Pignac-Kobinger and Irina Fernandez.

References

1. Holyst MM, Hoffman RW. U-small nuclear ribonucleoprotein (RNP)-reactive autoantibodies: diagnostic testing and clinical interpretation. Clin Immunol Newsl 1998;18:53–55.
2. Hoffman, RW. Overlap syndromes: mixed connective tissue disease and Sjögren's syndrome. In: Lahita, RG., editor. Systemic Lupus Erythematosus. 4th. Academic Press; New York: 2004. p. 717-744.
3. Hoffman, RW. Mixed connective tissue disease and other connective tissue diseases. In: Wallace, DJ.; Hannahs Hahn, B., editors. Dubois Systemic Lupus Erythematosus. 7th. New York: 2007. p. 975-991.
4. Burdt MA, Hoffman RW, Deutscher SL, Wang GS, Johnson JC, Sharp GC. Long-term outcome in mixed connective tissue disease: longitudinal clinical and serologic findings. Arthritis Rheum 1999;42:899–909. [PubMed: 10323445]
5. Kramer A. The structure and function of proteins involved in mammalian pre-mRNA splicing. Annu Rev Biochem 1996;65:367–409. [PubMed: 8811184]
6. Pettersson I, Hinterberger M, Mimori T, Gottlieb E, Steitz JA. The structure of mammalian small nuclear ribonucleoproteins: identification of multiple protein components reactive with anti-(U1) ribonucleoprotein and anti-Sm autoantibodies. J Biol Chem 1984;259:5907–5914. [PubMed: 6232278]
7. Hinterberger M, Pettersson I, Steitz JA. Isolation of small nuclear ribonucleoproteins containing U1, U2, U4, U5, and U6 RNAs. J Biol Chem 1983;258:2604–2613. [PubMed: 6185498]
8. Query CC, Bentley RC, Keene JD. A common RNA recognition motif identified within a defined U1 RNA binding domain of the 70K U1 snRNP protein. Cell 1989;57:89–101. [PubMed: 2467746]
9. Kaneoka H, Hsu KC, Takeda Y, Sharp GC, Hoffman RW. Molecular genetic analysis of HLA-DR and HLA-DQ genes among anti-U1–70-kd autoantibody positive connective tissue disease patients. Arthritis Rheum 1992;35:83–94. [PubMed: 1370621]
10. Cervino ACL, Tsinoremas NF, Hoffman RW. A genome-wide study of lupus: preliminary analysis and data release. Ann NY Acad Sci 2007;1110:131–139. [PubMed: 17911428]
11. Hoffman RW, Takeda Y, Sharp GC, Lee DR, Kaneoka H, Caldwell CW. Human T cell clones reactive against U-small nuclear ribonucleoprotein autoantigens from connective tissue disease patients and healthy individuals. J Immunol 1993;151:6460–6469. [PubMed: 8245479]
12. Holyst MM, Hill DL, Hoch SO, Hoffman RW. Analysis of human T cell and B cell responses against U small nuclear ribonucleoprotein 70-k, B and D polypeptides among patients with systemic lupus erythematosus and mixed connective tissue disease. Arthritis Rheum 1997;40:1493–1503. [PubMed: 9259431]
13. Greidinger EL, Gazitt T, Jaimes KF, Hoffman RW. Human T cell clones specific for heterogeneous nuclear ribonucleoprotein A2 autoantigen from connective tissue disease patients assist in autoantibody production. Arthritis Rheum 2004;50:2216–2222. [PubMed: 15248220]
14. Hoffman RW. T cells in the pathogenesis of systemic lupus erythematosus. Clin Immunol 2004;113:4–13. [PubMed: 15380523]
15. Talken BL, Lee DR, Caldwell CW, Quinn TP, Schäfermeyer KR, Hoffman RW. Analysis of T cell receptors specific for U1–70-kD small nuclear ribonucleoprotein autoantigen: the α chain

complementarity determining region three is highly conserved among connective tissue disease patients. Hum Immunol 1999;60:200–208. [PubMed: 10321956]

16. Talken BL, Bailey CW, Reardon SL, Caldwell CW, Hoffman RW. Structural analysis of TCR α and β chains from human T-cell clones specific for small nuclear ribonucleoprotein polypeptides Sm-D, Sm-B and U1–70 kDa: TCR complementarity determining region 3 usage appears highly conserved. Scand J Immunol 2001;54:204–210. [PubMed: 11439168]
17. Greidinger EL, Foecking MF, Schäfermeyer KR, Bailey CW, Primm SL, Lee DR, Hoffman RW. T cell immunity in connective tissue disease patients targets the RNA binding domain of the U1–70-kD small nuclear ribonucleoprotein. J Immunol 2002;169:3429–3437. [PubMed: 12218166]
18. Ito K, Brian HH, Molina M, Han J, Magram J, Saar E, Belunis C, Bolin DR, Arceo R, Campbell R, et al. HLA-DR4-IE chimeric class II transgenic, murine class II-deficient mice are susceptible to experimental allergic encephalitis. J Exp Med 1996;183:2635–2644. [PubMed: 8676084]
19. Greidinger EL, Foecking MF, Magee J, Wilson L, Ranatunga S, Ortmann RA, Hoffman RW. A major B cell epitope present on the apoptotic but not the intact form of the U1-70-kDa ribonucleoprotein autoantigen. J Immunol 2004;172:709–716. [PubMed: 14688384]
20. Greidinger EL, Zang Y, Jaimes K, Hogenmiller S, Nassiri M, Bejarano P, Barber GN, Hoffman RW. A murine model of mixed connective tissue disease induced with U1 small nuclear RNP autoantigen. Arthritis Rheum 2006;54:661–669. [PubMed: 16453294]
21. Greidinger EL, Hoffman RW. The appearance of U1 RNP antibody specificities in sequential autoimmune human antisera follows a characteristic order that implicates the U1–70 kd and B′/B proteins as predominant U1 RNP immunogens. Arthritis Rheum 2001;44:368–375. [PubMed: 11229468]
22. Hoffman RW, Sharp GC, Deutscher SL. Analysis of anti-U1 RNA antibodies in patients with connective tissue disease: association with HLA and clinical manifestations of disease. Arthritis Rheum 1995;38:1837–1844. [PubMed: 8849357]
23. McMurray RW, Hoffman RW, Tang H, Braley-Mullen H. T cell receptor Vβ usage in murine experimental autoimmune thyroiditis. Cell Immunol 1996;172:1–9. [PubMed: 8806800]
24. Cornberg M, Chen AT, Wilkinson LA, Brehm MA, Kim SK, Calcagno C, Ghersi D, Puzone R, Celada F, Welsh RM, Selin LK. Narrowed TCR repertoire and viral escape as a consequence of heterologous immunity. J Clin Invest 2006;116:1443–1456. [PubMed: 16614754]
25. Sonderstrup G, Cope AP, Patel S, Congia M, Hain N, Hall FC, Parry SL, Fugger LH, Michie S, McDevitt HO. HLA class II transgenic mice: models of the human $CD4^+$ T-cell immune response. Immunol Rev 1999;172:335–343. [PubMed: 10631958]
26. Forsthuber TG, Shive CL, Wienhold W, de Graff K, Spack EG, Sublett R, Melms A, Kort J, Racke MK, Weissert R. T cell epitopes of human myelin oligodendrocyte glycoprotein identified in HLA-DR4 (DRB1*0401) transgenic mice are encephalitogenic and are presented by human B cells. J Immunol 2001;167:7119–7125. [PubMed: 11739534]
27. Madsen LS, Andersson EC, Jansson L, Krogsgaard M, Andersen CB, Engberg J, Strominger JL, Svejgaard A, Hjorth JP, Holmdahl R, et al. A humanized model for multiple sclerosis using HLA-DR2 and a human T-cell receptor. Nat Genet 1999;23:343–347. [PubMed: 10610182]
28. Dudek NL, Maier S, Chen ZJ, Mudd PA, Mannering SI, Jackson DC, Zeng W, Keech CL, Hamlin K, Pan ZJ, et al. T cell epitopes of the Ls/SSB autoantigen in humanized transgenic mice expressing the HLA class II haplotypes DRB1*0301/DQB1*0201. Arthritis Rheum 2007;56:3387–3398. [PubMed: 17907193]
29. Hoffman RW, Greidinger EL, Zang Y. $CD4^+$ T cells reactive with U1–70-kD autoantigen can transfer disease and are central to pathogenesis in new murine model of lupus. Clin Immunol 2007;123:S83. Abstract.
30. Monneaux F, Muller S. Key sequences involved in spreading of the systemic autoimmune response to spliceosome proteins. Scand J Immunol 2001;54:45–54. [PubMed: 11439147]
31. Mamula MJ, Fatenejad S, Craft J. B cells process and present lupus autoantigens that initiate autoimmune T cell responses. J Immunol 1994;152:1453–1461. [PubMed: 8301145]
32. Monneaux F, Pariette V, Briand JP, Muller S. Intramolecular T cell spreading in unprimed MRL/*lpr* mice. Arthritis Rheum 2004;50:3232–3228. [PubMed: 15476231]

33. Monneaux F, Hoebeke J, Sordet C, Nonn C, Briand JP, Maillere B, Sibillia J, Muller S. Selective modulation of $CD4^+$ T cells from lupus patients by a promiscuous, protective peptide analogue. J Immunol 2005;175:5839–5847. [PubMed: 16237076]
34. Talken BL, Schäfermeyer KR, Bailey CW, Lee DR, Hoffman RW. T cell epitope mapping of the Smith autoantigen reveals that highly conserved Smith antigen motifs are the dominant target of T cell immunity in systemic lupus erythematosus. J Immunol 2001;167:562–568. [PubMed: 11418695]
35. Talken BL, Holyst MM, Lee DR, Hoffman RW. T cell receptor β-chain third complementarity-determining region gene usage is highly restricted among Sm-B autoantigen-specific human T cell clones derived from patients with connective tissue disease. Arthritis Rheum 1999;42:703–709. [PubMed: 10211884]
36. Davies TF, Martin A, Concepscion ES, Graves P, Cohen L, Ben-Nun A. Evidence for limited variability of antigen receptors on in-trathyroidal T cells in autoimmune thyroid disease. N Engl J Med 1991;325:238–244. [PubMed: 1829139]
37. Chott A, Probert CS, Gross GG, Blumberg RS, Balk SP. A common TCR β-chain expressed by $CD8^+$ intestinal mucosa T cells in ulcerative colitis. J Immunol 1996;156:3024–3035. [PubMed: 8609425]
38. Mantegazza R, Andreetta F, Bernasconi P, Baggi F, Oksenberg JR, Simoncini O, Mora M, Cornelio F, Steinman L. Analysis of T cell receptor repertoire of muscle-infiltrating T lymphocytes in polymyositis. J Clin Invest 1993;91:2880–2886. [PubMed: 8514895]
39. Hoffman RW. T-cell directed therapy in systemic lupus erythematosus. Future Rheumatol 2006;1:597–605.

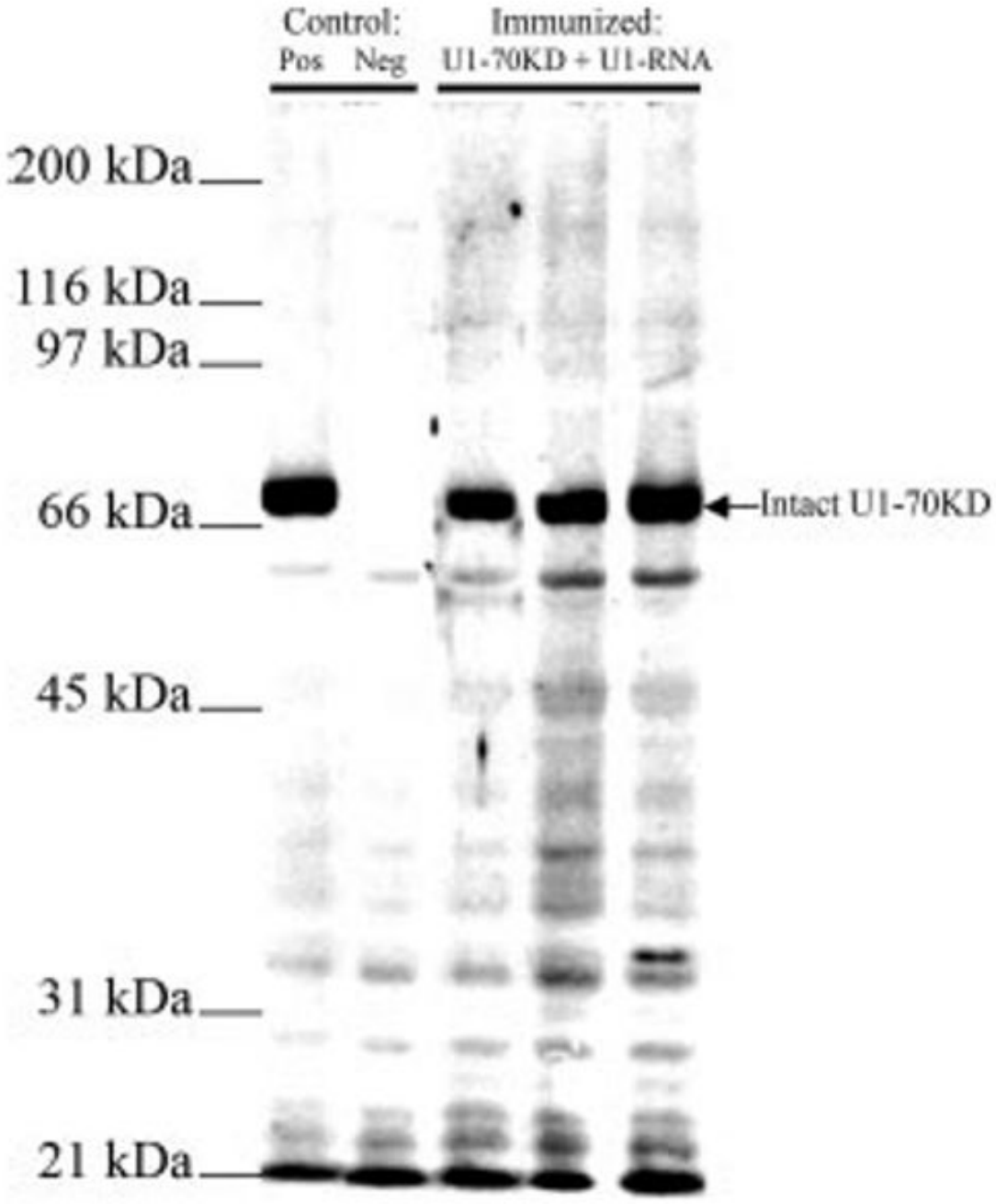

FIGURE 1.

Immunoblot of sera from immunized mice and controls. IgG anti-70-kDa Abs detected by immunoblotting of Jurkat extract using sera from 70-kDa/U1-RNA-immunized HLA-DR4-Tg mice which were diluted 1/5000. *Lane 1*, A positive control serum; *lane 2*, A serum from an unimmunized HLA-DR4-Tg mouse; *lanes 3–5*, sera from HLA-DR4-Tg-immunized mice. Prominent reactivity with 70 kDa is clearly detectable following immunization (*lanes 3–5*) along with several additional weaker autoantibody reactivities of undefined specificity.

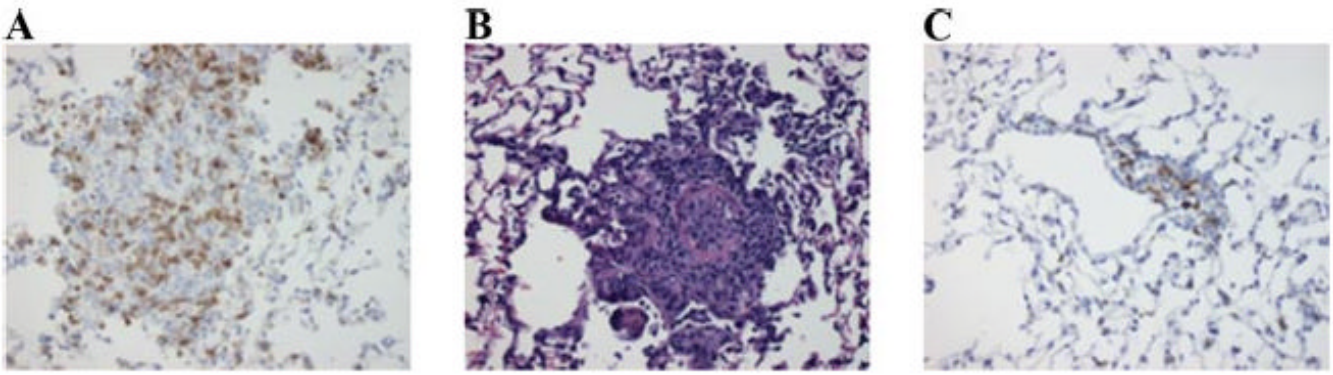

FIGURE 2.

Lung histologic findings in the 70-kDa/U1-RNA-immunized HLA-DR4-Tg murine model. *A*, H&E staining of representative lung tissue demonstrating mononuclear cell infiltration of the lung. *B*, Section of lung corresponding to *A* which was stained immunohistochemically using enzyme-conjugated anti-CD3 mAb demonstrating abundance of T cells within inflammatory lesions. *C*, A representative section of lung from a naive unimmunized HLA-DR4-Tg mouse demonstrating the absence of detectible T cell infiltration in unimmunized mice.

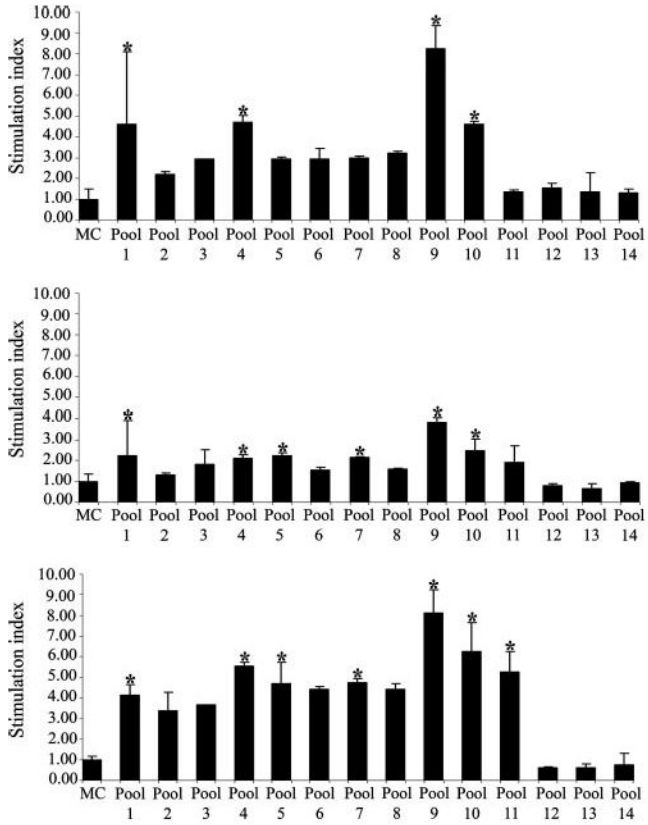

FIGURE 3.

Murine $CD4^+$ T cells proliferate to 70-kDa Ag-peptide pools. Shown are results from three mice using purified $CD4^+$ T cells incubated with a series of individual overlapping peptides spanning the 70-kDa protein in the presence of irradiated syngeneic APC. After 48 h of culture [^{3}H]thymidine was added to each well and after an additional 18 h, cells were harvested and [^{3}H]thymidine incorporation was measured by scintillation counting. The horizontal line indicates a stimulation index (SI) of 1.5 as a baseline comparison for all three experiments shown. There were seven regions identified that typically had substantially higher SI as measured by [^{3}H]thymidine incorporation. Indicated by an asterisk (*), these seven regions reacted strongly with $CD4^+$ T cells from 70-kDa/U1-RNA-immunized mice. Results are shown in comparison to MC proliferation for T cells cultured with APCs in the absence of added peptides. Error bars illustrate 2 SD above the mean.

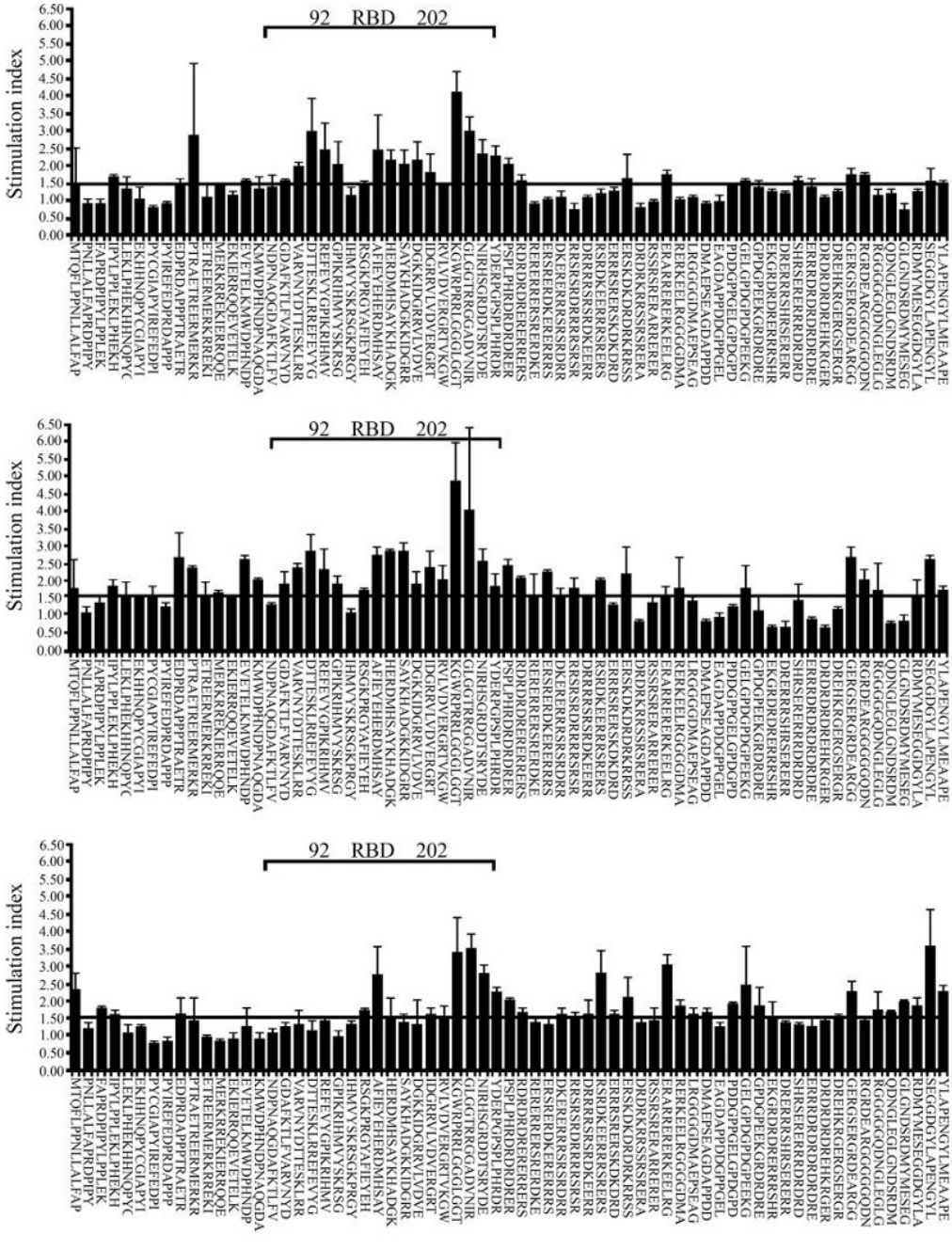

FIGURE 4.

Murine CD4$^+$ T cell response to individual 70-kDa peptides. Purified CD4$^+$ T cells were incubated with a series of individual peptides, overlapping in sequence, spanning the entire 70-kDa protein in the presence of irradiated APC. The [^{3}H]thymidine incorporation was measured, stimulation index was calculated, and a representative result from each of three individual mice shown. Error bars illustrate 2 SD above the mean. The majority of the stimulatory T cell epitopes resided within the RBD, shown in brackets.

Table I

TRBV primers

TRBV Gene Name	TCR V*β* Family	Primer Sequence
TRBV1	V*β*2	ATGAGCCAGGGCAGAACCTTGTAC
TRBV2	V*β*4	CTAAAGCCTGATGACTCGGCCACA
TRBV3	V*β*16	CTGAAAATCCAACCCACAGCACTGG
TRBV4	V*β*10	CTTCGAATCAAGTCTGTAGAGCCGG
TRBV5	V*β*1	CCAGACAGCTCCAAGCTACTTTTAC
TRBV12-1	V*β*5.2	CCTTGGAACTGGAGGACTCTGCTA
TRBV12-2	V*β*5.1	CTTGGAGCTAGAGGACTCTGCCG
TRBV13-1	V*β*8.3	ATTGGCTTCTCCCTCTCAGACATCTT
TRBV13-2	V*β*8.2	GCTACCCCCTCTCAGACATCAGTG
TRBV13-3	V*β*8.1	GGCTTCCCTTTCTCAGACAGCTGTA
TRBV14	V*β*13	CAAGATCCAGTCTGCAAAGCAGGG
TRBV15	V*β*12	CTCTGAAGATTCAACCTACAGAACCC
TRBV16	V*β*11	GAAGATCCAGAGCACGCAACCCC
TRBV17	V*β*9	CTCTCTCTACATTGGCTCTGCAGG
TRBV19	V*β*6	GCCCAGAAGAACGAGATGGCCGTT
TRBV20	V*β*15	AAATGCATATCTTGAAGACAGAGGCTTA
TRBV23	V*β*20	CACTCTGCAGCCTGGGAATCAGAA
TRBV24	V*β*17	CTCTGAAGAAGACGACTCAGCACTG
TRBV26	V*β*3	AGAAATTCAGTCCTCTGAGGCAGGA
TRBV29	V*β*7	CTGGATTCTGCTAAAACAAACCAGAC
TRBV30	V*β*18	GCAAGGCCTGGAGACAGCAGTATC
TRBV31	V*β*14	CACGGAGAAGCTGCTTCTCAGCC
TRBC	C*β*	GGCCAAGCACACGAGGGTAGCCT

Table II

Peptide pool sequences

Pool		Sequence
1	70K.M.1.15	MTQFLPPNLLALFAP
	70K.P.7.15	PNLLALFAPRDPIPY
	70K.F.13.15	FAPRDPIPYLPPLEK
	70K.I.19.15	IPYLPPLEKLPHEKH
	70K.L.25.15	LEKLPHEKHHNQPYC
2	70K.E.31.15	EKHHNQPYCGIAPYI
	70K.P.37.15	PYCGIAPYIREFEDP
	70K.P.43.15	PYIREFEDPRDAPPP
	70K.E.49.15	EDPRDAPPPTRAETR
	70K.P.57.15	PTRAETREERMERKR
3	70.K.E.61.15	ETREERMERKRREKI
	70K.M.67.15	MERKRREKIERRQQE
	70K.E.73.15	EKIERRQQEVETELK
	70K.E.81.15	EVETELKMWDPHNDP
	70K.K.87.15	KMWDPHNDPNAQGDA
4	70K.N.93.15	NDPNAQGDAFKTLFV
	70K.G.99.15	GDAFKTLFVARVNYD
	70K.V.107.15	VARVNYDTTESKLRR
	70K.D.113.15	DTTESKLRREFEVYG
	70K.R.121.15	REFEVYGPIKRIHMV
5	70K.G.127.15	GPIKRIHMVYSKRSG
	70K.I.132.15	IHMVYSKRSGKPRGY
	70K.R.139.15	RSGKPRGYAFIEYEH
	70K.A.147.15	AFIEYEHERDMHSAY
	70K.H.153.15	HERDMHSAYKHADGK
6	70K.S.159.15	SAYKHADGKKIDGRR
	70K.D.165.15	DGKKIDGRRVLVDVE
	70K.I.169.15	IDGRRVLVDVERGRT
	70K.R.173.15	RVLVDVERGRTVKGW
	70K.K.185.15	KGWRPRRLGGGLGGT
7	70K.G.195.15	GLGGTRRGGADVNIR
	70K.N.207.15	NIRHSGRDDTSRYDE
	70K.Y.219.15	YDERPGPSPLPHRDR
	70K.P.225.15	PSPLPHRDRDRDRER
	70K.R.231.15	RDRDRDRERERRERS

Pool		Sequence
8	70K.R.237.15	RERERRERSRERDKE
	70K.E.243.15	ERSRERDKERERRRS
	70K.D.249.15	DKERERRRSRSRDRR
	70K.R.255.15	RRSRSRDRRRRSRSR
	70K.D.261.15	DRRRRSRSRDKEERR
9	70K.R.267.15	RSRDKEERRRSRERS
	70K.E.273.15	ERRRSRERSKDKDRD
	70K.E.279.15	ERSKDKDRDRKRRSS
	70K.D.285.15	DRDRKRRSSRSRERA
	70K.R.291.15	RSSRSRERARRERER
10	70K.E.297.15	ERARRERERKEELRG
	70K.R.303.15	RERKEELRGGGGDMA
	70K.L.309.15	LRGGGGDMAEPSEAG
	70K.D.315.15	DMAEPSEAGDAPPDD
	70K.E.321.15	EAGDAPPDDGPPGEL
11	70K.P.327.15	PDDGPPGELGPDGPD
	70K.G.333.15	GELGPDGPDGPEEKG
	70K.G.339.15	GPDGPEEKGRDRDRE
	70K.E.345.15	EKGRDRDRERRRSHR
	70K.D.351.15	DRERRRSHRSERERR
12	70K.S.357.15	SHRSERERRRDRDRD
	70K.E.363.15	ERRRDRDRDRDRDRE
	70K.D.369.15	DRDRDRDREHKRGER
	70K.D.375.15	DREHKRGERGSERGR
	70K.G.381.15	GERGSERGRDEARGG
13	70K.R.387.15	RGRDEARGGGGGQDN
	70K.R.393.15	RGGGGGQDNGLEGLG
	70K.Q.399.15	QDNGLEGLGNDSRDM
	70K.G.405.15	GLGNDSRDMYMESEG
	70K.R.411.15	RDMYMESEGGDGYLA
14	70K.S.417.15	SEGGDGYLAPENGYL
	70K.Y.423.15	YLAPENGYLMEAAPE

Table III

Epitopes on UI-70-kDa autoantigen recognized by $CD4^+$ T cells

	$CD4^+$ T Cells Stimulated %	
Epitope	**Murine, *n* = 10**	**Human, *n* = 6**
1	30	16
2	60	16
3	40	32
4	30	16
5	30	83

Table IV

TRVB expression in CD4$^+$ T cells from immunized and naive mice

	U1-70-kDa-Immunized Mice		Naive Mice	
TCRVβ Family	**Mean %**	**SD**	**Mean %**	**SD**
2	2.5	±1.2	3.1	±1.3
3	5.0	±2.1	5.7	±2.5
4	6.5	±1.2	5.8	±2.1
5.1, 5.2	2.2	±0.9	2.6	±1.5
6	10.4	±1.0	11.3	±1.7
7	3.6	±0.9	4.8	±1.8
8.3	9.9	±2.3	8.4	±1.5
9	2.1	±1.4	2.2	±1.3
10	8.5	±0.4	9.8	±2.4
11	1.1	±0.7	1.3	±1.3
12	0.9	±1.4	1.5	±1.4
13	1.9	±1.1	1.8	±1.0
14	9.4	±1.7	9.7	±1.4
17	1.0	±0.9	1.8	±1.0

Table V

TCR deduced amino acid sequence from CD4$^+$ T cells isolated from U1-70-kDa-immunized HLA-DR4-transgenic mouse spleen

TRBV Gene Name	TCR Vβ Family	V	CDR3	J	TRBJ	No. of Isolates
TRBV5	Vβ1	CAS	SQGTNNNQAPL	FGEGTRLSVL	J1-5	3
		CAS	SPRARGYEQY	FGPGTRLTVL	J2-7	1
		CAS	SQDRGEQY	FGPGTRLTVL	J2-7	2
		CAS	SQEGTGGTLSYEQY	FGPGTRLTVL	J2-7	2
		CAS	SQGTGGNYAEQF	FGPGTRLTVL	J2-1	1
		CAS	SQDGTGSTQY	FGPGTRLLVL	J2-5	1
		CAS	SPGDSNERLF	FGHGTKLSVL	J1-4	1
		CAS	SQATGAQDTQY	FGPGTRLLVL	J2-5	1
		CAS	SQGANNQAPL	FGEGTRLSVL	J1-5	1
		CAS	SQRQGEVF	FGKGTRLTVV	J1-1	1
		CAS	SPRLGGNQDTQY	FGPGTRLLVL	J2-5	5
		CAS	SQEGWGGEDTQY	FGPGTRLLVL	J2-5	1
		CAS	SQDLGSGAETLY	FGSGTRLTVL	J2-3	1
TRBV1	Vβ2	CTC	SGGLGGREQY	FGPGTRLTVL	J2-7	2
		CTC	SAEARGSSDYT	FGSGTRLLVI	J1-2	1
		CTC	SASGTAYEQY	FGPGTRLTVL	J2-7	2
		CTC	TSTGGAREQY	FGPGTRLTVL	J2-7	1
		CTC	SALLNSDYT	FGSGTRLLVI	J1-2	1
		CTC	SVDRNTEVF	FGKGTRLTVV	J1-1	3
		CTC	SPGQNYAEQF	FGPGTRLTVL	J2-1	3
TRBV19	Vβ6	CAS	SIKGGGAEQF	FGPGTRLTVL	J2-1	1
		CAS	SMSEGSDYT	FGSGTRLLVI	J1-2	7
		CAS	SEWGADTGQLY	FGEGSKLTVL	J2-2	3
		CAS	SIKGQGYSDYT	FGSGTRLLVI	J1-2	1
		CAS	SPDRYEQY	FGPGTRLTVL	J2-7	1
		CAS	STTGGGEQY	FGPGTRLTVL	J2-7	1

TRBV Gene Name	TCR Vβ Family	V	CDR3	J	TRBJ	No. of Isolates
		CAS	SSDRQY	FGPGTRLTVL	J2-7	1
		CAS	SMRRTNQATQY	FGPGTRLLVL	J2-7	1
		CAS	SISQGPNERLF	FGHGTKLSVL	J1-4	1
		CAS	GTGFTEVF	FGKGTRLTVV	J1-1	1
		CAS	SIGGSSAETLY	FGSGTRLTVL	J2-3	1
		CAS	SIRLVNTLY	FGAGTRLSVL	J2-4	1
		CAS	SPTGNTLY	FGEGSRLIVV	J1-3	1
		CAS	STGFTEVF	FGKGTRLTVV	J1-1	1
TRBV13-3	Vβ8.1	CAS	RGQGGSPLY	FAAGTRLTVT	J1-6	6
		CAS	SHANTEVF	FGKGTRLTVV	J1-1	1
		CAS	NPNNYAEQF	FGPGTRLTVL	J2-1	1
		CVS	SDGQDTQY	FGPGTRLLVL	J2-5	1
		CAS	SARGQVSPLY	FAAGTWLTVT	J1-6	1
		CAK	LPGHENSDYT	FGSGTRLLVI	J1-2	1
		CAS	SRQGEETLY	FGSGTRLTVL	J2-3	1
		CAS	SEPTGGNYAEQF	FGPGTRLTVL	J2-1	1
		CAS	RPEHLNTGQLY	FGEGSKLTVL	J2-2	1
		CAS	SDQGSYNSPPY	FAAGTRLTVT	J1-6	1
		CAS	RPGHLNTGQLY	FGEGSKLTVL	J2-2	1
		CAS	RIAGTSSAETLY	FGSGTRLTVL	J2-3	1
		CAS	SDWGSDYT	FGSGTRLLVI	J1-2	3
		CAS	AKYNSPLY	FAAGTRLTVT	J1-6	1
		CAS	SDAGTVAEQF	FGPGTRLTVL	J2-1	1
		CAS	TPGHISNERLF	FGHGTKLSVL	J1-4	1
		CAS	SLRGSAETLY	FGSGTRLTVL	J2-3	1
TRBV13-2	Vβ8.2	CAS	GGLGGYEQY	FGPGTRLTVL	J2-7	3
		CAS	GDAGWGSSYEQY	FGPGTRLTVL	J2-7	1
		CAS	GGQGASPLY	FAAGTRLTVT	J1-6	1

TRBV Gene Name	TCR Vβ Family	V	CDR3	J	TRBJ	No. of Isolates
		CAS	GDAVESSYEQY	FGPGTRLTVL	J2-7	1
		CAS	GGTGGGYEQY	FGPGTRLTVL	J2-7	1
		CAS	GRDSYNSPLY	FAAGTRLTVL	J1-6	1
		CAS	GGLVSQNTLY	FGAGTRLSVL	J2-4	3
		CAS	GDAGRYNSPLY	FAAGTRLTVT	J1-6	1
		CAS	GSYEQY	FGPGTRLTVL	J2-7	1
		CAS	GDMGSSAETLY	FGSGTRLTVL	J2-3	1
		CAS	GRGPGNTLY	FGEGSRLIVV	J1-3	1
		CAS	GGIQDTQY	FGPGTRLLVL	J2-5	1
		CAS	GGDSNYAEQF	FGPGTRLTVL	J2-1	2
		CAS	GDAGTNNSPLY	FAAGTRLTVT	J1-6	1
		CAS	GRDWGSSAETLY	FGSGTRLTVL	J2-3	1
		CAS	GDATGSNERLF	FGHGTKLSVL	J1-4	1
TRBV13-1	Vβ8.3	CAS	SGQGPSAETLY	FGSGTRLTVL	J2-3	3
		CAS	SGTEYQDTQY	FGPGTRLLVL	J2-5	1
		CAS	SGRVAGNTLY	FGEGSRLIVV	J1-3	3
		CAS	SDFGQVPWNNQAPL	FGEGTRLSVL	J1-5	1
		CAS	TGTGDYEQY	FGPGTRLTVL	J2-7	1
		CAS	SDPGQLNYAEQF	FGPGTRLTVL	J2-1	1
		CAS	SSALGSAETLY	FGSGTRLTVL	J2-3	1
		CAS	SDSLGLPTLY	FGAGTRLSVL	J2-4	1
		CAS	SSLGGHYAEQF	FGPGTRLTVL	J2-1	1
		CAS	SGRDNYAEQF	FGPGTRLTVL	J2-1	1
		CAS	SGTGVYEQY	FGPGTRLTVL	J2-7	1
		CAS	SVGGALAETLY	FGSGTRLTVL	J2-3	1
		CAS	SERANTGQLY	FGEGSKLTVL	J2-2	1
		CAS	RPGQGRNTLY	FGAGTRLSVL	J2-4	2
		CAS	RGTNTEVF	FGKGTRLTVV	J1-1	1

TRBV Gene Name	TCR Vβ Family	V	CDR3	J	TRBJ	No. of Isolates
		CAT	RTGGSAETLY	FGSGTRLTVL	J2-3	2
		CAS	SNWGGEQY	FGPGTGLTVL	J2-7	1
		CAS	SREILYAEQF	FGPGTRLTVL	J2-1	1
		CAS	SDWDSGNTLY	FGEGSRLIVV	J1-3	1

Table VI

TCR deduced amino acid sequence from CD4$^+$ T cells isolated from U1-70-kDa-immunized HLA-DR4-transgenic mouse lung

TRBV Gene Name	TCR Vβ Family	V	CDR3	J	TRBJ	No. of Isolates
TRBV5	Vβ1	CAS	SLDRVANTEVF	FGKGTRLTVV	J1-1	1
		CAS	SQELLGVSAETLY	FGSGTRLTVL	J2-3	2
		CAS	SPQGDNNQAPL	FGEGTRLSVL	J1-5	1
		CAS	SPPEQY	FGPGTRLTVL	J2-7	1
TRBV12-2	Vβ5.1	CAS	SPGQGAYEQY	FGPGTRLTVL	J2-7	3
		CAS	SRDWGAGQLY	FGEGSKLTVL	J2-2	1
		CAS	SLGQGAAPLY	FAAGTRLTVT	J1-6	1
		CAS	SLGVINYAEQF	FGPGTRLTVL	J2-1	1
		CAS	SLRWGNYAEQF	FGPGTRLTVL	J2-1	1
		CAS	SLRGQGNSPLY	FAAGTRLTVT	J1-6	1
TRBV12-1	Vβ5.2	CAS	SLGWGRNTLY	FGAGTRLSVL	J2-4	1
		CAS	SLAWGPWAEQF	FGPGTRLTVL	J2-1	4
		CAS	SLPDGAETLY	FGSGTRLTVL	J2-3	1
		CAS	SLQGWDTLY	FGAGTRLSVL	J2-4	1
		CAS	SRTDSGNTLY	FGEGSRLIVV	J1-3	1
TRBV13-3	Vβ8.1	CAS	SAGVNTEVF	FGKGTRLTVV	J1-1	1
		CAS	SPGTGGDAETLY	FGSGTRLTVL	J2-3	1
		CAS	SDGGNYAEQF	FGPGTRLTVL	J2-1	1
		CAS	SAGQGGEQY	FGPGTRLTVL	J2-7	2
		CAS	SRQGAAEVF	FGKGTRLTVV	J1-1	1
TRBV13-2	Vβ8.2	CAS	GDAGTGVNERLF	FGHGTKLSVL	J1-4	1
		CAS	GDGLGVYEQY	FGPGTRLTVL	J2-7	1
		CAS	GPTGNYAEQF	FGPGTRLTVL	J2-1	1
		CAS	GDPWDYEQY	FGPGTRLTVL	J2-7	1
		CAS	GDWGTSAETLY	FGSGTRLTVL	J2-3	1
		CAS	GGQTSAETLY	FGSGTRLTVL	J2-3	1

TRBV Gene Name	TCR Vβ Family	V	CDR3	J	TRBJ	No. of Isolates
		CAS	GDAWTGDERLF	FGHGTKLSVL	J1-4	1
TRBV13-1	V*β*8.3	CAS	SDGAGGYNSPLY	FAAGTRLTVT	J1-6	4
		CAS	SDGGGVNYAEQF	FGPGTRLTVL	J2-1	1
		CAS	SDSGGNYAEQF	FGPGTRLTVL	J2-1	2
		CAS	SEGGSNYAEQF	FGPGTRLTVL	J2-1	1
		CAS	SDASRTNERLF	FGHGTKLSVL	J1-4	1
		CAS	SDWGGYEQY	FGPGTRLTVL	J2-7	2
		CAS	STESYSGNTLY	FGEGSRLIVV	J1-3	2
		CAS	SDASGTNERLF	FGHGTKLSVL	J1-4	1
TRBV4	V*β*10	CAS	SLQGSGNTLY	FGEGSRLIVV	J1-3	1
		CAS	SSGTGSYEQY	FGPGTRLTVL	J2-7	1
		CAS	TRLGESAETLY	FGSGTRLTVL	J2-3	1
		CAS	SHWGRNAEQF	FGPGTRLTVL	J2-1	1
		CAS	SSGQAANSDYT	FGSGTRLLVI	J1-2	1
		CAS	SLLGGQQDTQY	FGPGTRLLVL	J2-5	1
		CAS	SSGLGGYEQY	FGPGTRLTVL	J2-7	1
		CAS	SSRLGGYAEQF	FGPGTRLTVL	J2-1	1
TRBV16	V*β*11	CAS	SLGNSDYT	FGSGTRLLVI	J1-2	1
		CAS	SSDWGGAGNYAEQF	FGPGTRLTVL	J2-1	1
		CAS	SLGLGYEQY	FGPGTRLTVL	J2-7	1
		CAS	SPDWGVRNYAEQF	FGPGTRLTVL	J2-1	1
		CAS	SSGVGNTLY	FGEGSRLIVV	J1-3	1
TRBV31	V*β*14	CAW	SLGVSGNTLY	FGEGSRLIVV	J1-3	2
		CAW	TDWGDYAEQF	FGPGTRLTVL	J2-1	1
		CAW	SRLGGREQY	FGPGTRLTVL	J2-7	1
		CAW	SKLGDYAEQF	FGPGTRLTVL	J2-1	1
		CAW	SQGNSGNTLY	FGEGSRLIVV	J1-3	1
		CAW	SLTGGEVF	FGKGTRLTVV	J1-1	1

TRBV Gene Name	TCR Vβ Family	V	CDR3	J	TRBJ	No. of Isolates
		CAW	SPDSAETLY	FGSGIRLTVL	*J2-3*	1
		CAS	SRTSSTGQLY	FGEGSKLTVL	*J2-2*	4
TRBV3	*Vβ16*	CAS	SLDWGQNTLY	FGAGTRLSVL	*J2-4*	1
		CAS	SLPQGFSYEQY	FGPGTRLTVL	*J2-7*	1
		CAS	SRENQDTQY	FGPGTRLLVL	*J2-5*	1
		CAS	SSSYEQY	FGPGTRLTVL	*J2-7*	1
		CAS	SPRLGGGEQY	FGPGTRLTVL	*J2-7*	1
		CAS	SLVGEQY	FGPGTRLTVL	*J2-7*	1
		CAS	SFGDWGYEQY	FGPGTRLTVL	*J2-7*	1
		CAS	SLQNSNERLF	FGHGTKLSVL	*J1-4*	1

Table VII

Alignment of deduced amino acid sequences of human and murine TCR from 70-kDa T cells

Origin[a]		TRBV Sequences		J Region[b]
Human	CAS[c]	SQMGQGHYEQY	FGPGTRLTVT	2S7
	CAT	SGQGDYEQY	FGPGTRLTVT	2S7
	CAS	SMAGGREQF	FGPGTRLTVL	2S1
Murine Lung	CAS	GDGLGVYEQY	FGPGTRLTVL	2S7
	CAS	SSGLGGYEQY	FGPGTRLTVL	2S7
	CAS	SSGTGSYEQY	FGPGTRLTVL	2S7
	CAS	SAGQGGEQY	FGPGTRLTVL	2S7
	CAS	SPGQGAYEQY	FGPGTRLTVL	2S7
	CAS	SPRLGGGEQY	FGPGTRLTVL	2S7
	CAW	SRLGGREQY	FGPGTRLTVL	2S7
	CAS	SDWGGYEQY	FGPGTRLTVL	2S7
	CAS	SDGGNYAEQF	FGPGTRLTVL	2S1
	CAS	SSRLGGYAEQF	FGPGTRLTVL	2S1
Spleen	CAS	GGLGGYEQY	FGPGTRLTVL	2S7
	CAS	SQEGTGGTLSYEQY	FGPGTRLTVL	2S7
	CAS	SGTGVYEQY	FGPGTRLTVL	2S7
	CAS	SQGTGGNYAEQF	FGPGTRLTVL	2S1

[a] Human sequences are from T cell clones derived from mixed connective tissue disease patients (16). Murine sequences are from T cell lines generated using 70-kDa-immunized mice restimulated in vitro using 70 kDa as described in the text.

[b] Human BV: 7 of 18 (56%) used J2S7; murine lung BV: 19 of 81 (24%) used J2S7; murine spleen BV: 24 of 115 (21%) used J2S7.

[c] Sequences which were shared across all human and murine TRBV are underlined.